

Experimental Comparison between Nyquist-WDM and Continuous DFT-S-OFDM Systems

Chen Zhu⁽¹⁾, Bill Corcoran^(1,2), Arthur J. Lowery^(1,2)

⁽¹⁾ Monash University, Melbourne, Australia, chen.zhu@monash.edu

⁽²⁾ Centre for Ultrahigh-bandwidth Devices for Optical Systems (CUDOS), Australia.

Abstract We experimentally compare Nyquist-WDM and continuous DFT-S-OFDM systems with 16×64-Gb/s PDM-16QAM signals over 800-km SSMF. The DSP implementations of both systems with fractional oversampling rate are investigated, experimental results show that Nyquist-WDM system performs better with the same processing complexity.

Introduction

To cope with the ever increasing bandwidth demand for optical transmission, high-order quadrature-amplitude-modulation (QAM) in combination with very densely packed wavelength division multiplexing (WDM) channels could realize high spectral efficiency transmission schemes¹.

Nyquist pulse shaping is widely employed to generate near-rectangular spectrum for each wavelength in WDM systems (N-WDM) to minimize inter-channel-interference^{1,2}. Discrete Fourier transform spread OFDM (DFT-S-OFDM) has been demonstrated to be an effective method for generating Nyquist-like sub-bands, while alleviating the high peak-to-average-ratio (PAPR) drawback of conventional OFDM^{3,4}. To the best of our knowledge, there is no previous work directly comparing these two systems, which motivates this paper.

In this paper we discuss both the transmitter and receiver digital signal processing (DSP) requirements of N-WDM and continuous DFT-S-OFDM (C-DFT-S-OFDM) systems with a fractional oversampling rate. The computational complexity, efficiency of the receiver structure and implementation issues are investigated. Both systems are demonstrated in a 1.024-Tb/s polarization division multiplexed (PDM) 16QAM experiment. We show that N-WDM achieves better performance due to higher stop-band attenuation under limited computational effort.

Generation and reception of Nyquist-WDM and C-DFT-S-OFDM

Figure 1 shows the transmitter side DSP that generates N-WDM and single-band C-DFT-S-OFDM. For N-WDM, Nyquist pulse shaping is first implemented in the frequency-domain with a 2× oversampling rate. After symbol mapping and serial-to-parallel (S/P) block packing, FFT is used to convert each block's signals into the frequency domain. Typically for each block, the original K-size signals are upsampled by a factor of two, then a 2K-point FFT is applied. By noting

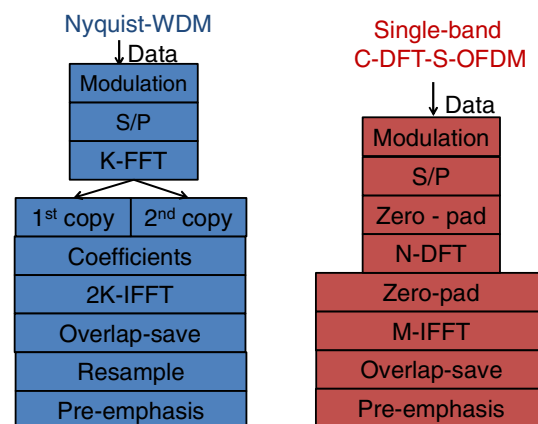


Fig. 1: Generation of Nyquist-WDM and single-band C-DFT-S-OFDM systems

that the FFT of the upsampled signal is actually repeating the FFT of the original K-point signal twice, the same result can be achieved by taking a K-point FFT of the original signal and cascading the two copies of it, to reduce the computational effort. After the FFT, frequency domain root-raise-cosine (RRC) taps are applied, followed by a 2K-point IFFT and 50% overlap-save to obtain the time-domain signals. The signals are resampled to a desired fractional oversampling rate (1.25 in the experiment) to maximize the baud rate output from a given digital to analog converter (DAC). Finally, a pre-emphasis filter compensates the frequency roll-off of the DAC and I/Q modulator.

Unlike a traditional DFT-S-OFDM system, which uses guard intervals after the IFFT operation^{3,4}, the generation of continuous DFT-S-OFDM (C-DFT-S-OFDM) system uses zero-padding before the DFT ($N/2$ zeros for each block) and 50% overlap-save after the IFFT to form the continuous outputs⁵. When only a single-band is defined, the transmitter DSP structure of C-DFT-S-OFDM is very similar to Nyquist-WDM except that there are no frequency domain coefficients that need to be multiplied. The oversampling rate is defined as N/M , therefore the oversampling rate of C-DFT-

S-OFDM can be tuned flexibly by adjusting the DFT/IFFT size accordingly. It is worth noting that, if fractional oversampling rate is required, the DFT size cannot be set to a power of 2 for efficient FFT processing (with fixed IFFT size).

As a smaller oversampling rate leads to closer spaced image frequency components, a proper electrical low-pass filter is necessary at the output of the DAC to remove those spurious frequency components. For both systems, a larger block size leads to a higher stop band attenuation and therefore better receiver sensitivity. The N-WDM system is able to control the number of RRC taps for a given stop band attenuation by adjusting the roll-off factor (at the cost of lowering the spectral efficiency), while C-DFT-S-OFDM cannot. Therefore, C-DFT-S-OFDM typically requires a relatively larger block size to produce a close-to-rectangular spectrum. For a fair comparison in our experiment, we set $2K=512$ with 0.01 roll-off for N-WDM, $N=408$ and $M=512$ for C-DFT-S-OFDM.

The receiver DSP for both systems are depicted in Fig. 2. Besides frequency offset compensation (FOC), linear channel equalization and phase recovery, a N-WDM system would typically require another RRC filter as matched filter, while for C-DFT-S-OFDM an M -point FFT is required as symmetric operation to the M -point IFFT operation at the transmitter. Computationally efficient processing for N-WDM system combines the matched filtering and linear equalization in a single multiple-input multiple-output frequency-domain equalizer (MIMO-FDE)⁶. C-DFT-S-OFDM can also use MIMO-FDE to remove linear channel impairments immediately after the FFT operation. Therefore both systems share a similar receiver processing structure.

For this scheme, FOC must be conducted

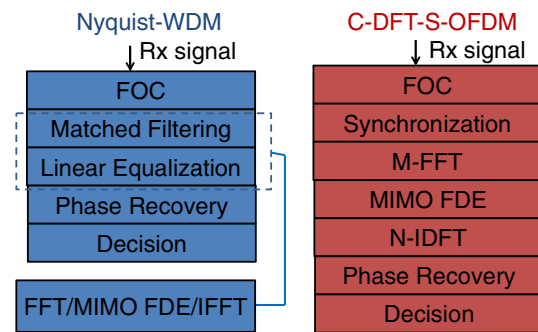


Fig. 2: Reception of Nyquist-WDM and single-band C-DFT-S-OFDM systems

first, otherwise neither a matched filter nor an M -point FFT can be correctly matched to the original RRC filter or M -point IFFT. However, N-WDM system has the flexibility to place the FOC function after linear equalization, by using an adaptive equalizer with increased equalizer tap length which also converges to a matched filter, while C-DFT-S-OFDM cannot and so be more sensitive to large frequency offset variance.

Experimental demonstration

Figure 3 shows the experimental setup. The transmitter uses eight ECLs with 16.3-GHz carrier spacing. The laser outputs were multiplexed with an 8×1 polarization-maintaining (PM) coupler followed by a wavelength selective switch (WS - Finisar Waveshaper) for power equalization. The baseband signals were defined as N-WDM (inset *i*) or C-DFT-S-OFDM (inset *ii*) signals using a 10-Gsample/s arbitrary waveform generator (AWG), which generates an 8-Gbaud signal. The AWG outputs are low-pass filtered and amplified, before driving the optical I/Q modulator to modulate the optical carriers. The spectrum of generated half-filled spectrum is shown as inset (*iii*) of Fig.3. This signal is then split into two paths: one path was frequency shifted by 8.15 GHz, amplified and

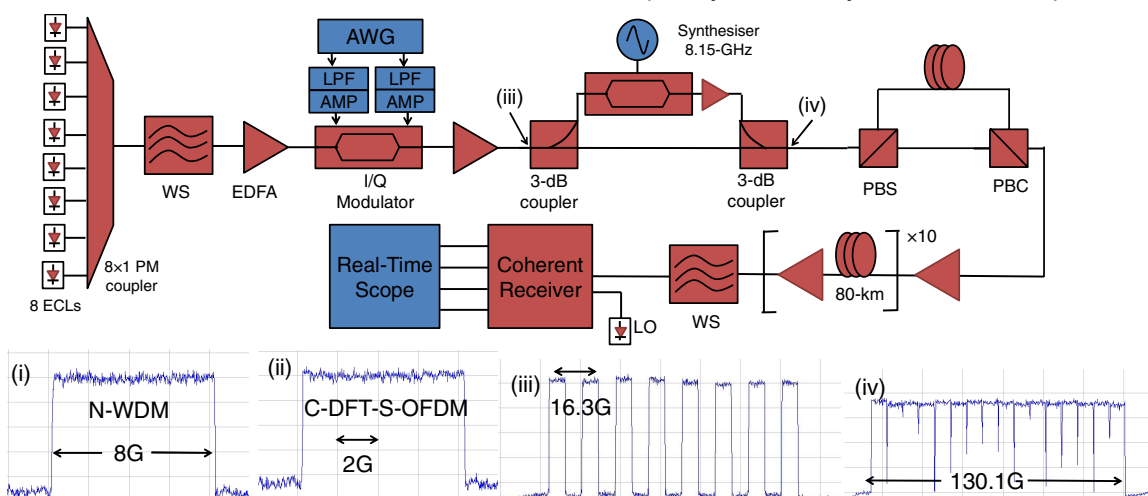


Fig. 3: Experimental setup. ECL: external cavity laser, WS: WaveShaper, LPF: electrical low-pass filter/amplifier, AMP: electrical low-pass filter, EDFA: Erbium-doped fiber amplifiers, PBS/PBC: polarization beam splitter/combiner.

recombined with the other path. This formed an even-odd channel structure for a continuous 130.1-GHz Nyquist-shaped super-channel (inset *iv*) transmission with 1.024-Tb/s total data rate. PDM was emulated by polarization split, delay in one polarization, then recombine. The optical signal was transmitted through a 10×80-km EDFA-amplified dispersion unmanaged link. Another WS was used to select the bands for coherent detection, and finally a real-time oscilloscope was used to digitize the signals for offline processing. The offline DSP for N-WDM system is as in⁶, and training-aided channel estimation⁷ is applied in C-DFT-S-OFDM system to set up the MIMO FDE taps.

Figure 4 shows the signal quality Q^2 -factors derived from measured BER using $Q^2(dB) = 20 \log_{10}(\sqrt{2} \operatorname{erfc}^{-1}(2BER))$, versus launch power for the 9th band of the super-channel. N-WDM shows clear a 0.8-dB advantage over C-DFT-S-OFDM, at the optimal launch power 4-dBm. This is due to the fact that with the same transmitter side computational complexity (*i.e.* same block size), the stop band attenuation of N-WDM with RRC pulse shaping is much deeper than that of DFT-S-OFDM system (comparing insets *(i)* and *(ii)* of Fig.3). The equalized constellation diagrams for both systems at 4-dBm launch powers are shown as two insets in Fig. 4. The fiber nonlinearity penalty is quite similar for both systems, as both systems have similar PAPRs with same roll-off. However, since the C-DFT-S-OFDM system is able to define multiple sub-bands for each carrier and modulator, it has the ability to be designed for an optimal baud rate (around 4-Gbaud^{3,8}) for super-channel transmission while still fully utilizing the DAC rate and the bandwidth of commercial modulators.

Fig. 5 shows the Q^2 values for all the channels after 800 km at the optimal launch power for the N-WDM and C-DFT-S-OFDM systems. For both systems, all channels were below the hard FEC limit of 3.8×10^{-3} (8.52-dB Q^2). On average, N-WDM outperforms C-DFT-

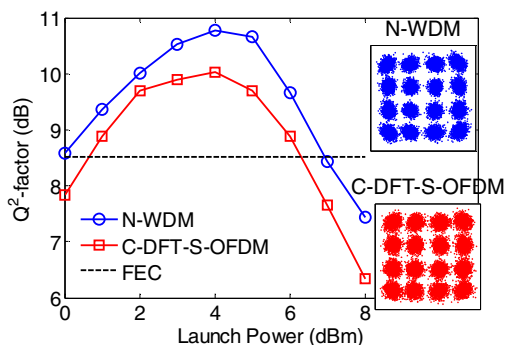


Fig. 4: Measured Q^2 value versus launch powers.

S-OFDM system by about 0.5-dB.

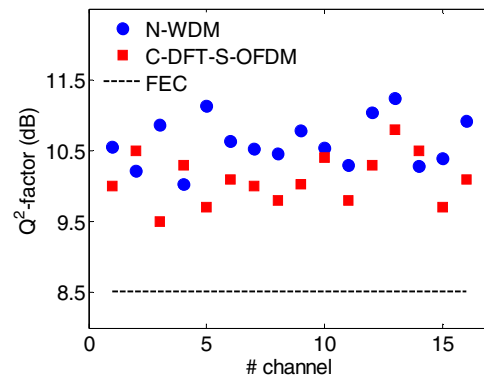


Fig. 5: Result for each channel at optimal launch power.

Conclusions

We have investigated methods for implementing super-channel transmission with N-WDM and C-DFTS-OFDM. These share similar DSP structures. We demonstrate both systems in a 1.024-Tb/s PDM-16QAM experiment over 800-km SSMF; the results show that N-WDM outperforms a C-DFTS-OFDM design that has similar computational complexity, due to its higher stop band attenuation.

Acknowledgements

This work was funded by an ARC Laureate Fellowship (FL130100041).

References

- [1] G. Bosco et al., "On the performance of Nyquist-WDM terabit superchannels based on PM-BPSK, PM-QPSK, PM-8QAM or PM-16QAM subcarriers," *J. Lightwave Technol.*, Vol. **29**, no. 1, p. 53 (2011).
- [2] R. Schmogrow et al., "Real-time Nyquist pulse generation beyond 100 Gbit/s and its relation to OFDM," *Opt. Express*, Vol. **20**, no. 1, p. 317 (2012).
- [3] Y. Tang et al., "DFT-spread OFDM for fiber nonlinearity mitigation," *IEEE Photonics Technol. Lett.*, Vol. **22**, no. 16, p. 1250 (2010).
- [4] X. Chen et al., "Experimental demonstration of improved fiber nonlinearity tolerance for unique-word DFT-spread OFDM systems," *Opt. Express*, Vol. **19**, no. 27, p. 26198 (2011).
- [5] L. B. Du et al., "Multi-channel generation and reception of Nyquist-WDM using digital DFTs," *Proc. OECC*, MR1-4, Tokyo (2013).
- [6] C. Zhu et al., "1.15 Tb/s Nyquist PDM 16-QAM Transmission with Joint Matched Filtering and Frequency-Domain Equalization," in *Proc. OFC*, Th4D.4, San Francisco (2014).
- [7] C. Zhu et al., "Low-Complexity Fractionally-Spaced Frequency Domain Equalization with Improved Channel Estimation for Long-Haul Coherent Optical Systems," in *Proc. OFC*, OW4B.5, Anaheim, (2013).
- [8] L. B. Du et al., "Optimizing the subcarrier granularity of coherent optical communications systems," *Opt. Express*, Vol. **19**, no.9, 8079-8084 (2011).